

Technical Documentation

MIT Maker Portfolio
Sidharth Baskaran, January 2022

About

This document serves to provide insight into the design process and highlight the 3 main engineering devices I have designed and built during high school as part of Science Olympiad. I chose to compete in these events out of interest—the physics of flight, materials science, and the complex nature of engineering problems were intriguing and rewarding to explore.

In general, [Science Olympiad](#) engineering events represent a multivariable problem with many solutions, approached through the construction of a physical device or contraption. The device must satisfy specific dimensional or mechanical constraints in order to compete against other devices. The winning device achieves the best metric—e.g. accuracy or flight time—against other competing teams. I will cover 3 such engineering events I found success in—Wright Stuff, Boomilever, and Gravity Vehicle—going in-depth about the design process, materials used, challenges faced, and any future plans if applicable.

[Wright Stuff](#)

[Objective](#)

[Aircraft](#)

[Rubber motors](#)

[Phugoid oscillations](#)

[Materials](#)

[Other challenges](#)

[Resources Used](#)

[Results](#)

[Boomilever](#)

[Objective](#)

[Design, materials and force analysis](#)

[Challenges](#)

[Gravity Vehicle](#)

[Objective](#)

[Vehicle](#)

[Chassis and axle mount](#)

[Chassis frame](#)

[Axle assembly](#)

[Ramp](#)

[Calibration](#)

[Materials](#)

[Challenges](#)

[V3 design](#)

Wright Stuff

I worked on Wright Stuff in the 2016-17, 2017-18, 2019-20, and 2020-21 Science Olympiad seasons, and plan on continuing in the 2021-22 (current) season. For the 2016-17 and 2017-18 seasons (under middle school Division B rules), I designed my aircraft using a 2D CAD software. For later seasons (high school Division C rules), I used the [Freedom Flight Models](#) kit.

Note about kit usage: Many teams adopted this strategy for Division C, and I also made the switch to building from a kit to maintain a competitive edge.

- The Freedom Flight design's leverage of laser-cut parts and mathematically optimized designs is hard to replicate on the amateur level.
- Despite the kit design not being original, I found that it was necessary to make custom modifications to achieve desired flight behavior.
- Further, I did not gain significant advantages in the trimming process due to usage of a kit, as this process is inherently difficult and independent of the aircraft's design.

Objective

To design, construct, and test free-flight rubber-powered monoplanes to achieve the maximum flight time aloft ([2020 Rules Manual](#)). There are essentially two stages of preparation I followed each season:

- **Designing/building the aircraft.** Initially the most time-consuming step, but less so over experience. Required great precision, patience, and diligence.
- **Finding a suitable flying area and successfully trimming the aircraft.** Always the most time-consuming step. Over the last 5 years, I've found school gyms to be the best flying locations as the air conditioning can be controlled.

Aircraft

The aircraft is a lightweight monoplane constructed using balsa wood, carbon fiber, cyanoacrylate glue, and mylar film. The design constraints, which have varied over the years, generally include:

- A minimum aircraft between 7 and 8 grams
- A limitation on the maximum propeller diameter
- Maximum dimension constraints for the aircraft's wing and rear stabilizer
- Material constraints include no pre-glued joints from kits, or the use of boron filaments

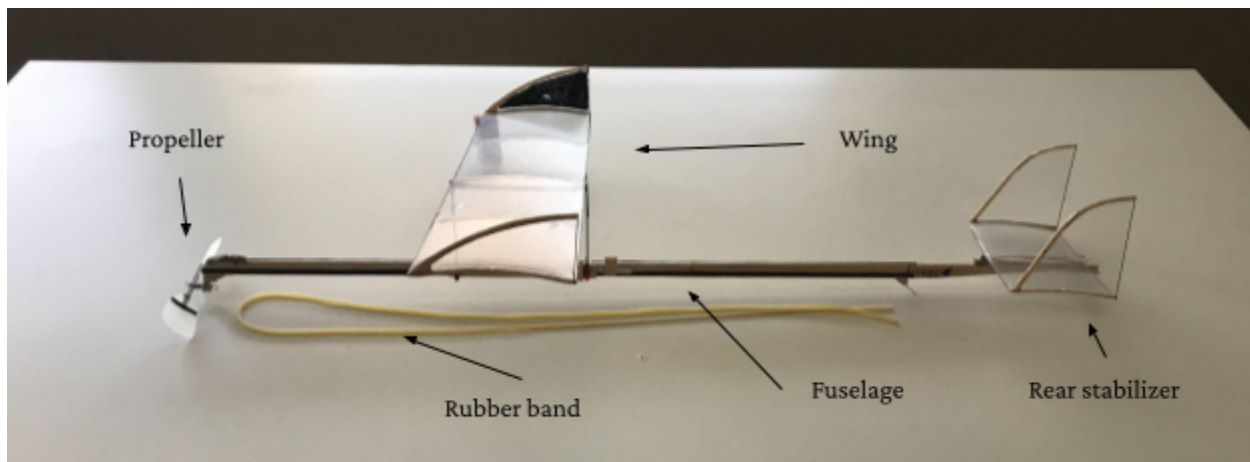


Figure 0: Wright Stuff aircraft diagram

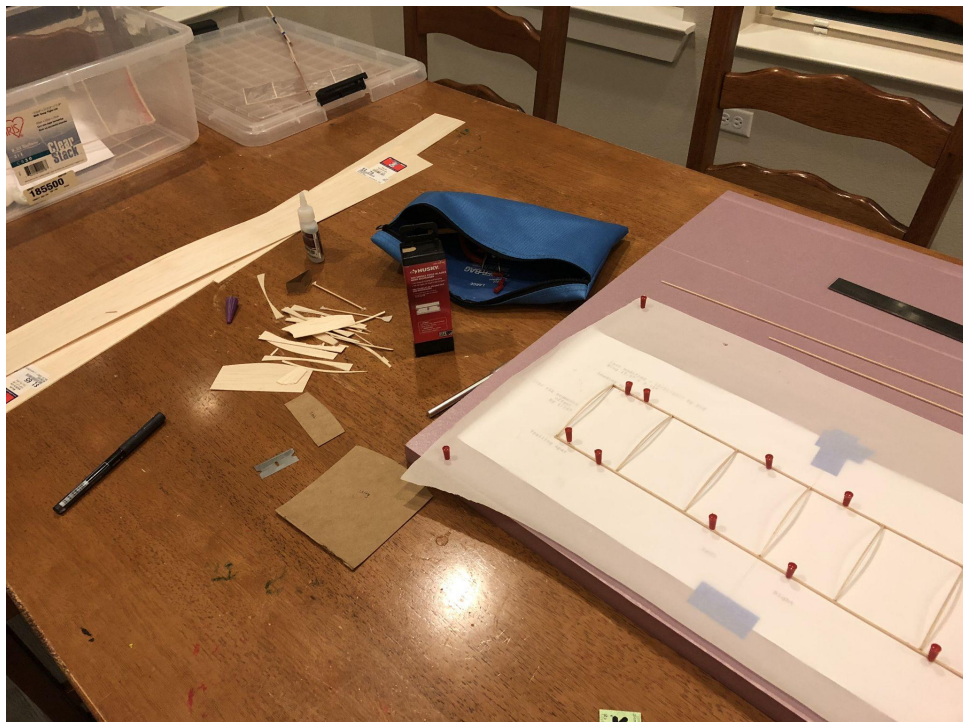
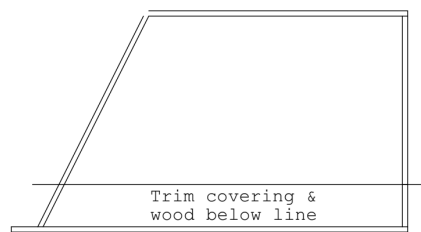
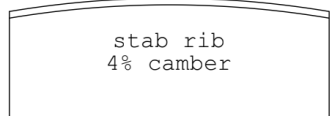


Figure 1: Construction phase of my design, circa 2017

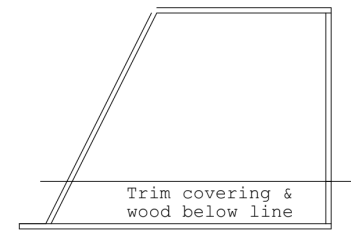
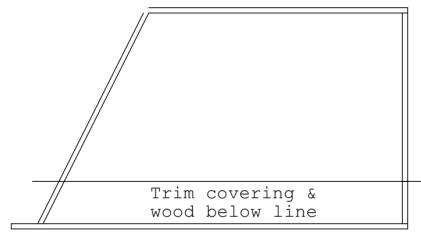


Figure 2: Preparing aircraft for flight at 2020 MIT invitational

Last modified - 12/25/2017
Rib template



Last modified - 12/26/2017
Wing tips, stab tip

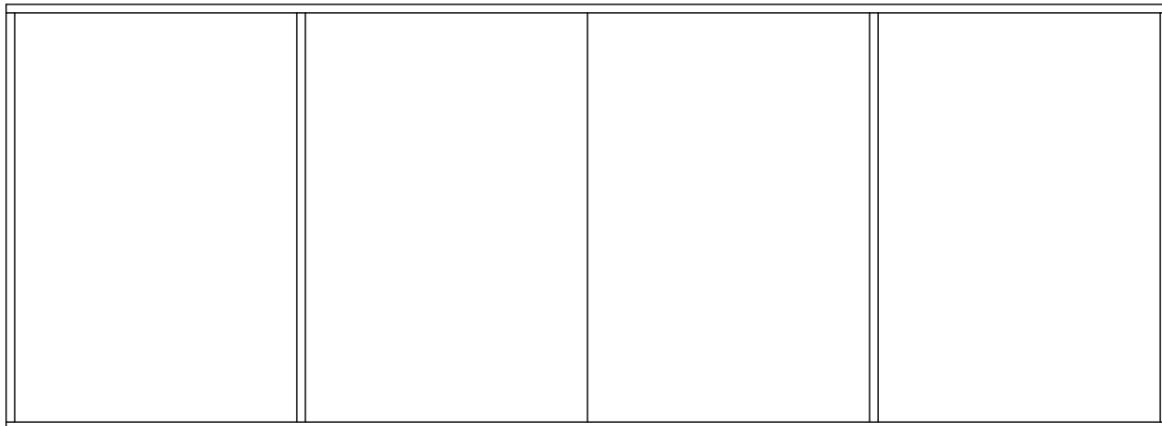


Wing tip

Stab tip

Last modified - 12/26/2017
Stab

Stab 8.5" x 3.125"
Leading spar



Trailing spar Left Right

Figure 3: 2017 design [Top left] Wing/stabilizer camber [Top right] Stabilizer and wingtips [Bottom] Rear stabilizer



Figure 4: Close-up of aircraft used in 2020 season, built with materials from Freedom Flight Kit

Rubber motors

Rubber motors are the sole means of propulsion for the aircraft

- They are attached via small bearings and hooks to the fuselage, and spin the lightweight propeller at a velocity which decreases at a variable rate.
- The rubber is winded using a special 15:1 gearbox-driven hand crank. My aircraft used special flight rubber branded as “Tan Super Sport” cut to precise widths of 1/16” or 3/32”.
- Each type and size of rubber has a different torque curve that gives it desirable properties for different aircraft.

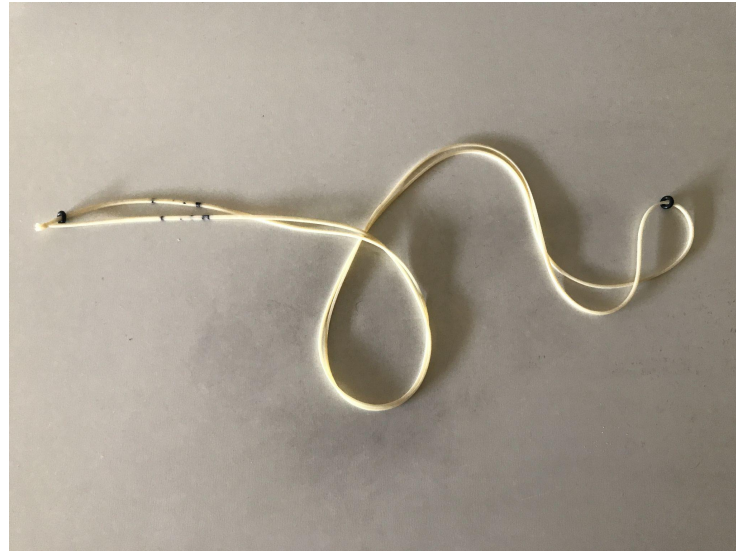


Figure 6: Rubber band close-up, notice the o-ring on each end

More winds equates to higher launch torque on the rubber band, but this can be calibrated using the rubber band's hysteresis property.

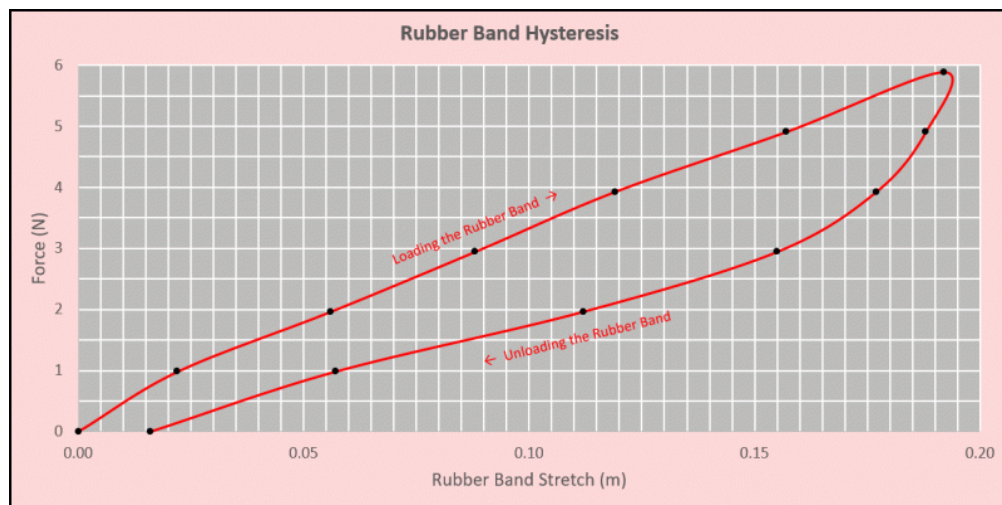


Figure 5: Hysteresis of rubber bands (image from [Pocket Lab](#)) when loading (winding) and unloading (unwinding).

A solution to the high-torque issues I encountered lay in “winding back” just prior to launching the aircraft. From empirical observation, I found that even 3-5 winds in the opposite direction lead to a significant reduction in launch torque.

Phugoid oscillations

A major issue I encountered was overcorrection of the aircraft in the vertical direction.

- The aircraft enters a highly unstable pattern of stalls followed by nosedives
- Observed as a positive feedback loop that decreases flight times by eventually inducing drag and deviation from the intended flight path.
- Cause ended up being a large decalage—difference in angles of attack (AOA) between the rear stabilizer and wing.

- I found that having the wing's angle of attack slightly more positive than the rear stabilizer offered the most stability, along with moving the plane's center of gravity in small increments to achieve the best performance.

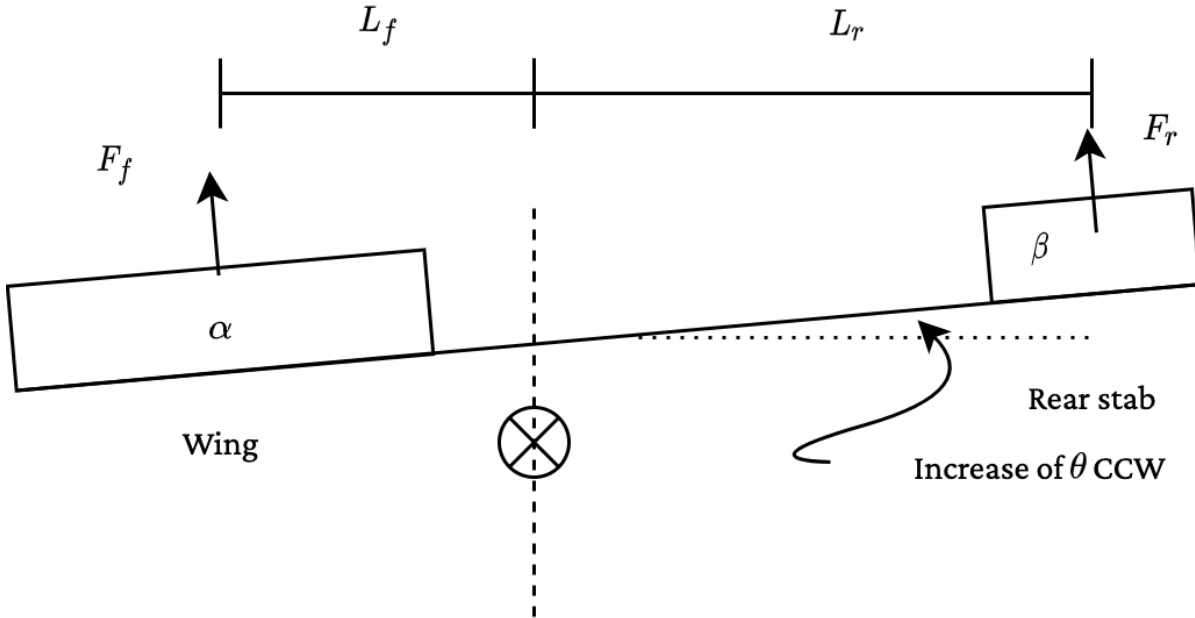


Figure 7: Phugoid oscillation diagram

A simplified take on what causes phugoid oscillations involves looking at the angles of attack (AoA) of the wing and rear stabilizers.

- Let us first assume that when the airplane is at static equilibrium (i.e. level flight) when $\theta = 0$.
- This means that the net torque induced by lift forces about the center of gravity (indicated by vertical dotted line) is 0.
- The wing AoA is α and rear stab has an AoA of β where $\alpha > \beta$.
- If we induce some perturbation θ in the counterclockwise direction as indicated in Figure 7, it follows that the wing AoA decreases to $\frac{\alpha - \theta}{\alpha} = 1 - \frac{\theta}{\alpha}$ and the rear stab AoA decreases by $\frac{\beta - \theta}{\beta} = 1 - \frac{\theta}{\beta}$.
- Clearly, the rear stabilizer's angle of attack has decreased by a larger percentage since $\frac{\theta}{\beta} > \frac{\theta}{\alpha}$. This allows equilibrium to be restored through a negative feedback system.

If we had induced a clockwise impulse instead, the condition of $\alpha > \beta$ would cause the rear stabilizer's AoA to *increase* by a greater factor than the wing. The negative-feedback loop occurs. If the constraint was flipped, we would have a positive feedback system that encourages phugoid oscillations.

Materials

- The chief material used to construct the plane was balsa wood and has many interesting properties that make it the most popular material for use in free-flight model construction. Firstly, it is light and soft, available in very low densities, making it suitable for precision modeling with minimal toolwork. In my aircraft, the fuselage was constructed with higher density balsa than the rest of

the model, given that it repeatedly bears the greatest torsional and compression load under the tension of a rubber band.

- To provide strength against crashes, the leading/trailing edges of all flight surfaces and parts of the fuselage were made with carbon fiber rods.
- The flight surfaces are covered with Mylar film
- Parts are bonded using medium-viscosity cyanoacrylate (CA) glue and 3M Super-77 spray glue

Other challenges

- **Consistency.** Between aircrafts of the same design, there were significant variations that were hard to notice physically, but accentuated in flight. The solution was to develop a sound trimming strategy to ensure that every plane could attain a similar flight behavior in case the primary aircraft was lost in an accident.
- **Finding a suitable flying area.** School gymsnasiums are the optimal environment, but are unfortunately restrictive in access. This emphasized the importance of thinking through my design and simulating the trimming process—even before throwing the plane into the air.
- **Transportation.** My solution was to delicately secure the aircraft in a Tupperware or plastic storage box using pieces of tape and foam. The entire box was then placed in a large suitcase and padded with foam inserts. Impressively, it was able to withstand tosses on the airport conveyor belt and full 360° range of movement.

Resources Used

I used a variety of online resources to learn about construction, trimming, and flight theory. The following were foundational to my success:

- freeflight.org
- Hip Pocket Aeronautics Forum
- Chuck Markos' construction tips

Results

The rules varied across the five seasons I have competed in this event. When the design constraints allowed for larger aircraft and propellers, flight times naturally increased. My aircraft have performed in a range of times from 1.5 to 2.5 minutes of endurance.

Boomilever

Objective

To design and construct a solely wooden cantilever structure capable of supporting an approximate point load on its end. The best design achieves the greatest structural efficiency (mass of load/mass of device). If the device holds over 15,000 grams, it receives a 5,000 gram bonus load added for a maximum possible load of 20,000 grams ([2020 Rules Manual](#)).



Figure 9: Loading boomilever with a sand, 2020 Regional Tournament (TAMU-SA)

Design, materials and force analysis

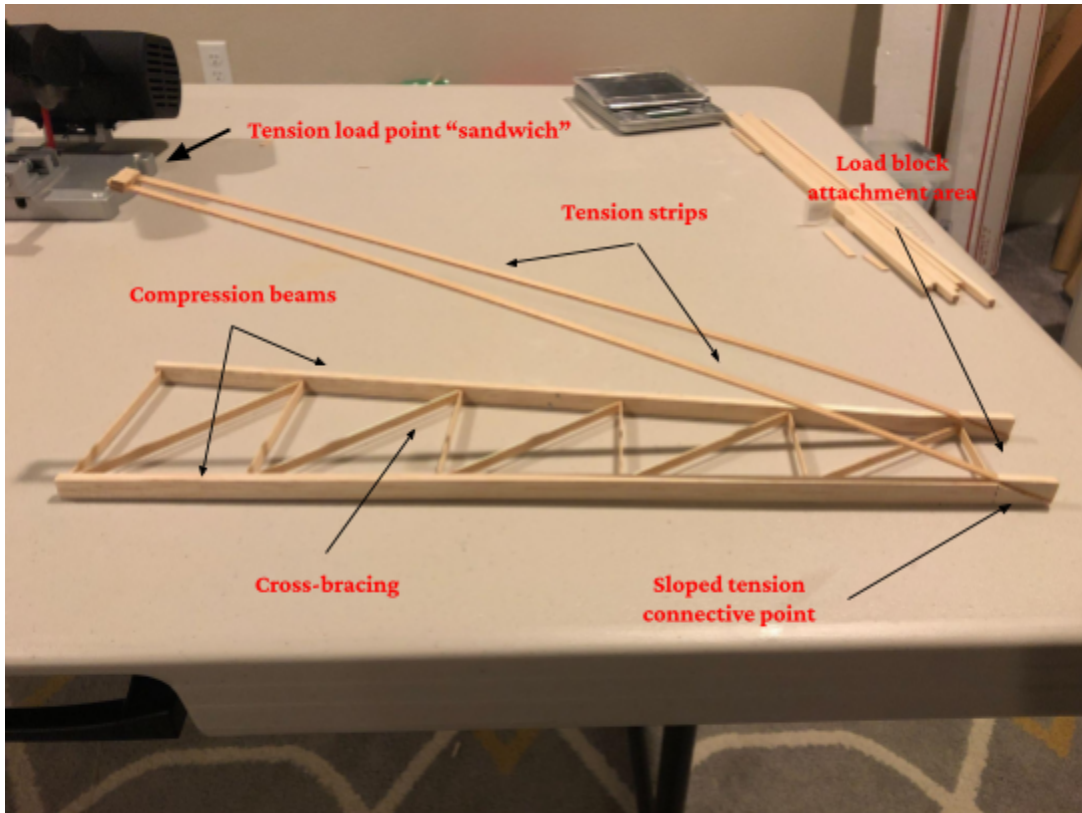


Figure 10: Labeled device image

- The device consists of the **compression** and **tension** sections, as indicated in Figure 10.
- In general, the tensile strength of wood is much greater than its compressive capability. Further, given the force analysis touched on the next section, the compressive force exerted on the device is greater than the tension experienced.
- My design focuses on reinforcing the compression members over the tension members:
 - **Compression:** composed of 2 large contiguous balsa beams linked via a simple crossing pattern of thin balsa strips. These thin connective strips, visible in Figure 10, serve to distribute the compressive load across the two beams but mainly as a structural choice to ensure the boomilever stays in one rigid piece.
 - **Tension:** composed of 2 thin strips of spruce or maple wood that slope down at the distal end below where the loading block is placed. They are connected at the J-hook mounting point using a glue-reinforced multi-layered maple strip “sandwich.”

The materials and tools used in construction and assembly of my boomilevers include:

- Autodesk AutoCAD to design printable plans
- Balsa sticks and sheets of many dimensions in medium density, sourced from Specialized Balsa Wood, LLC
- Precision-cut spruce and maple strips
- Cyanoacrylate glue, mini miter saw, and various small woodworking tools

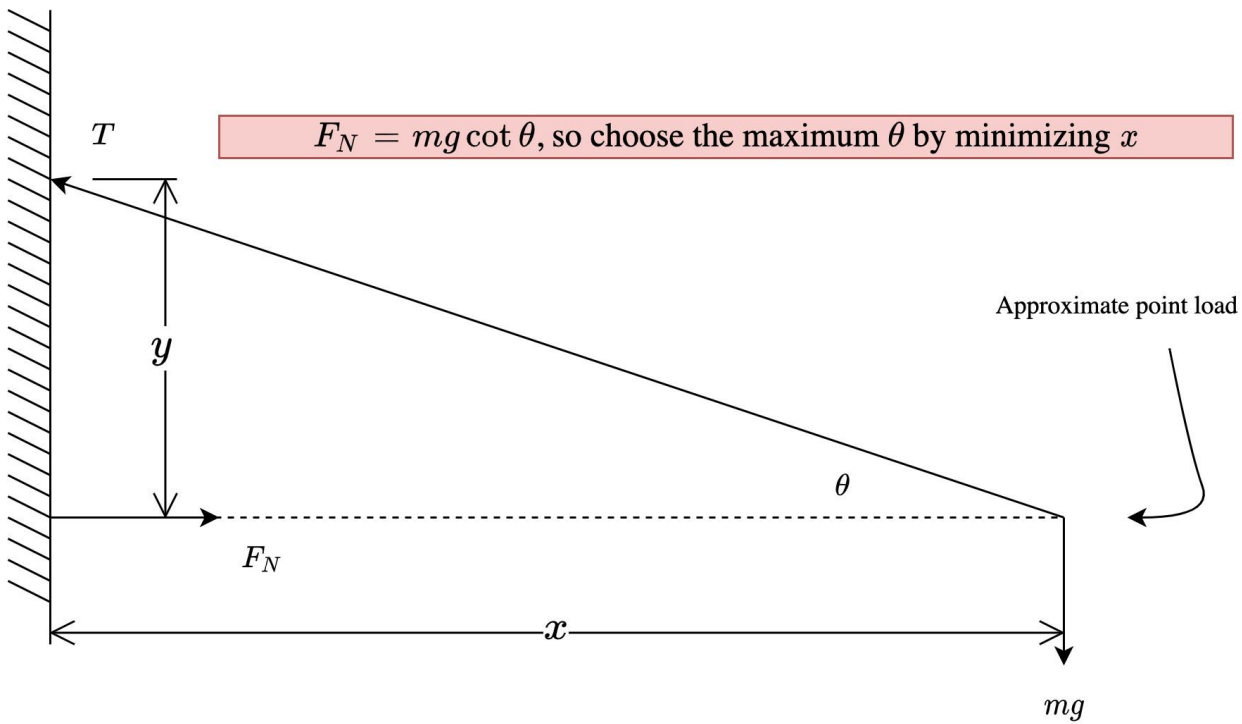


Figure 11: Simplified static force analysis

From Figure 11, we see that:

$$\begin{aligned} T \sin \theta &= mg, \quad T \cos \theta = F_N \\ F_N &= mg \cot \theta \end{aligned}$$

The tension-compression angle θ remains in the range $(0, \pi/4)$ in order to abide by design constraints provided in the Science Olympiad rules. My design attempted to minimize the compressive force (represented by F_N) by increasing θ .

- The below CAD design images (Figures 12, 13) are for the side and top views respectively while Figure 14 is a small design image of a “jig” I constructed to help match the vertical height between the J-hook mount point of the tension members and compression beams below.
- This is a critical aspect of the design, as improper alignment would result in torsion about an axis through the load point on the side view.
 - This could affect the distribution of the load on the device and lead to premature failure.

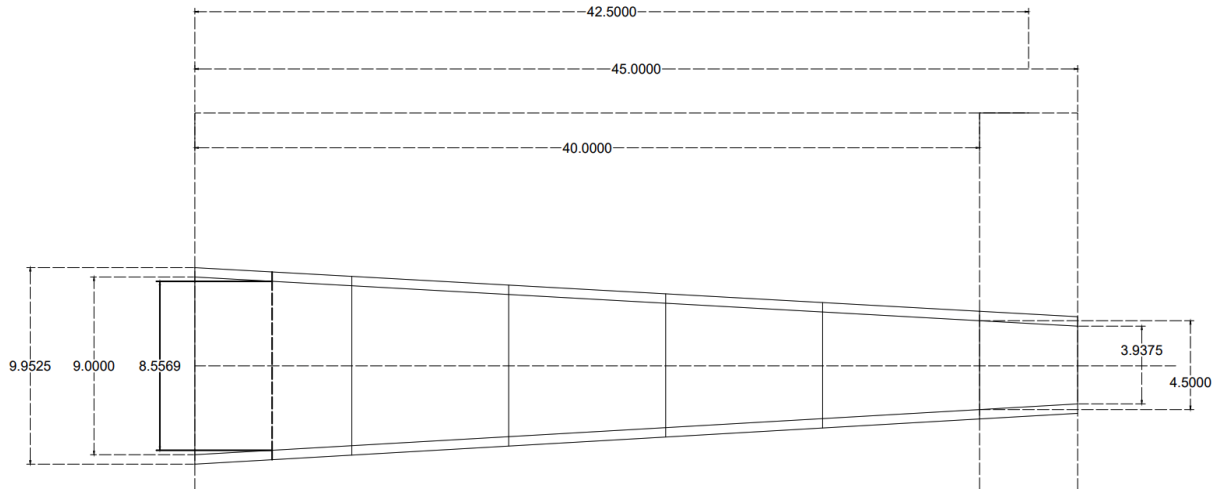


Figure 12.1: CAD Top view

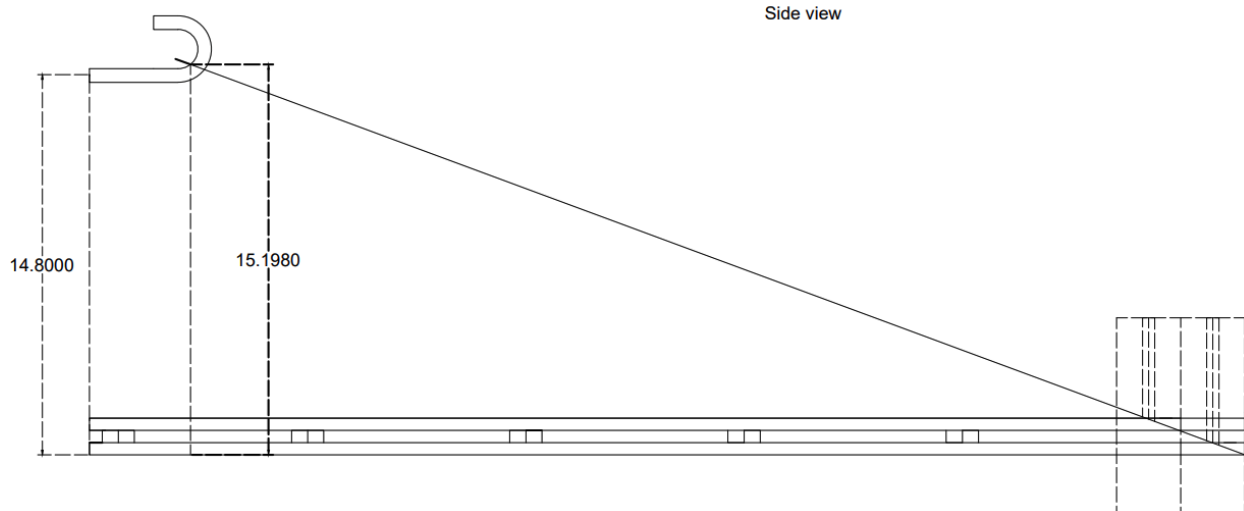


Figure 12.2: CAD Side view

Backwall frontview jig allows alignment
of tension members on either side of mounting bolt

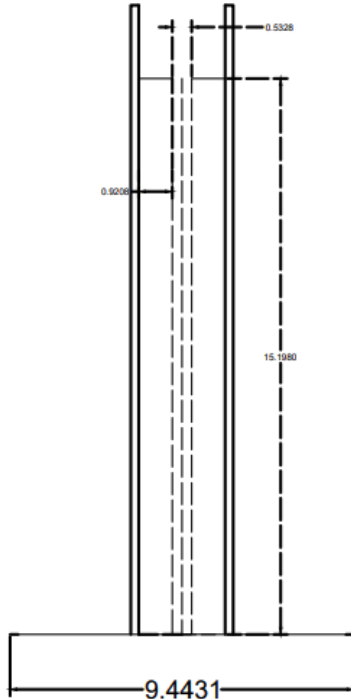


Figure 13: CAD of tension member mount jig

Challenges

- Weight consistency—important for efficiency—between designs was challenging to achieve due to the difficult nature of rationing and distributing cyanoacrylate glue usage. This was the main variable between designs. The other factor was the flat abuttal between the compression members and the mounting wall. This contact point required careful attention to detail, for asymmetry would lead to torsion in the compression members.
- Transportation of my device to tournaments posed little challenge due to the size and robust nature of the boomilever. For air travel, I utilized triangular postal mailing boxes within a plastic container to transport my primary device and a backup.

Gravity Vehicle

Objective

To design and construct a vehicle with gravitational potential energy being its sole source of propulsion, provided by an associated ramp which must also be designed and constructed by the competitor, to reach a predetermined stopping point as accurately as possible ([2021 Rules Manual](#)).

- The vehicle has a weight limit of 2 kg, and both the ramp and vehicle (in launch configuration) must fit within a rectangular prism of dimensions 100x50x50 cm.
- The target point, which is drawn on a centerline from the vehicle's start point, is between **2 and 5 meters from the start point**, necessitating that a robust braking and calibration mechanism be present on the vehicle.
- Also important to note from the rules is a $\frac{3}{8}$ inch dowel placed perpendicular to the track 1 meter from the start point.
- The design of my vehicle revolves around the complex nature of moving over this obstacle.

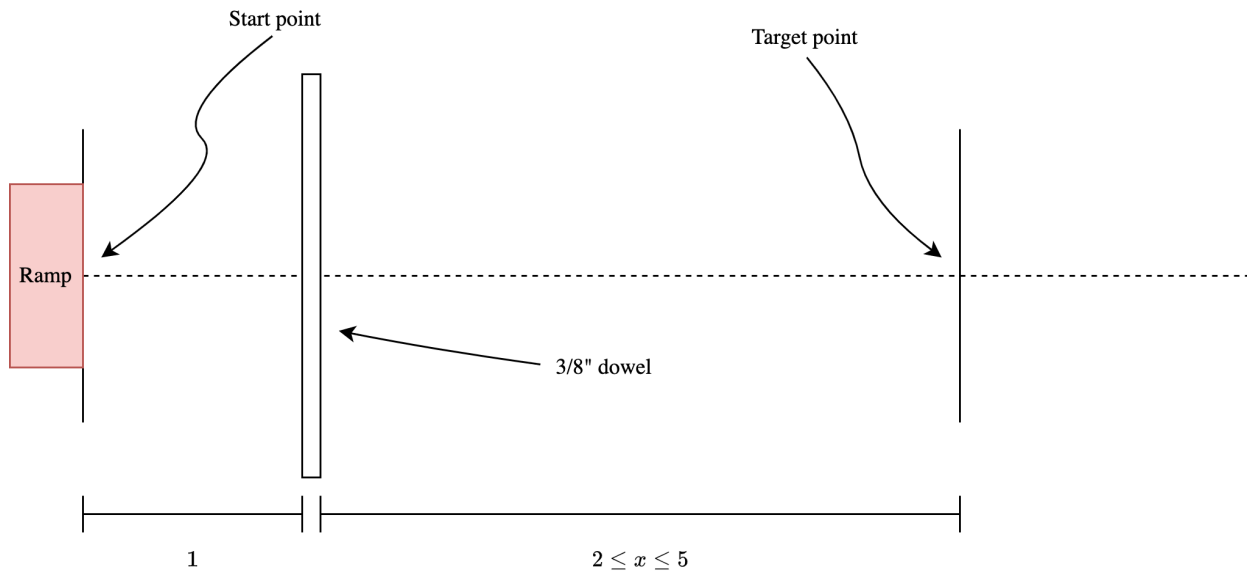


Figure 15: A simple layout of the track (all measurements in meters from the start point)

Vehicle

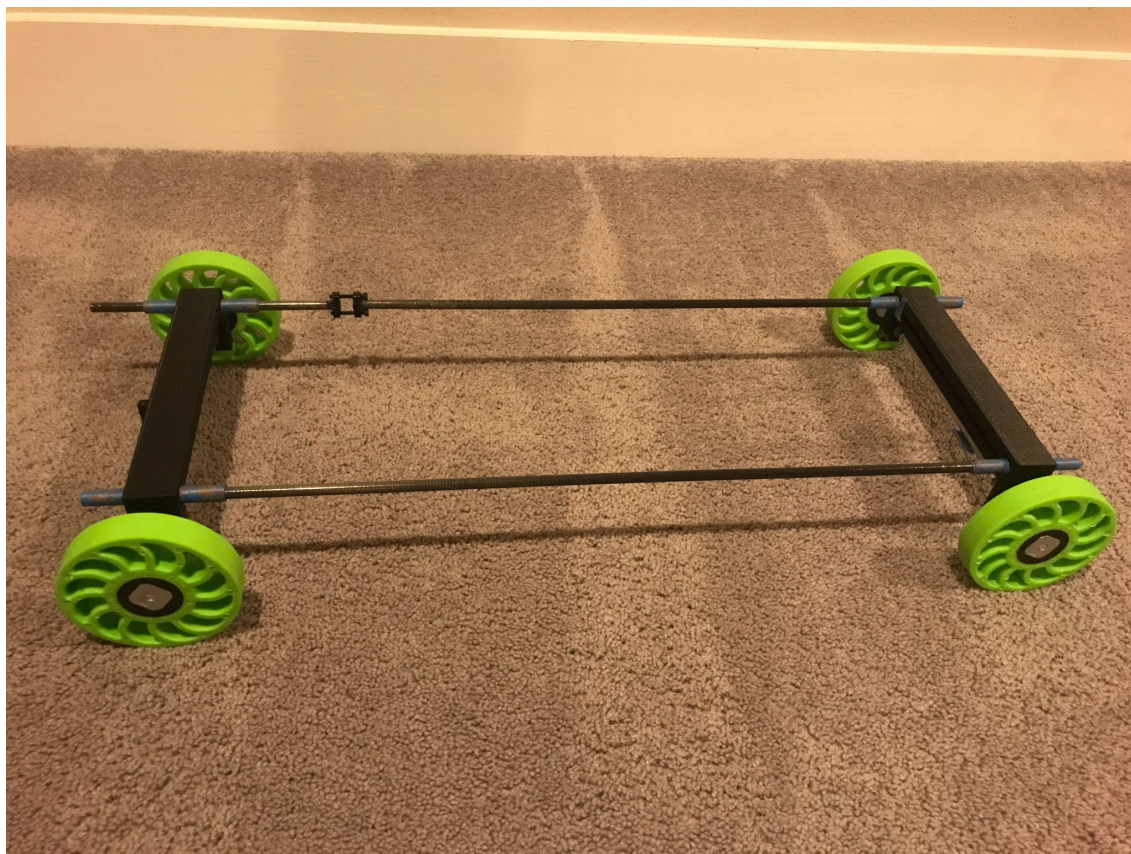


Figure 16: The V1 design

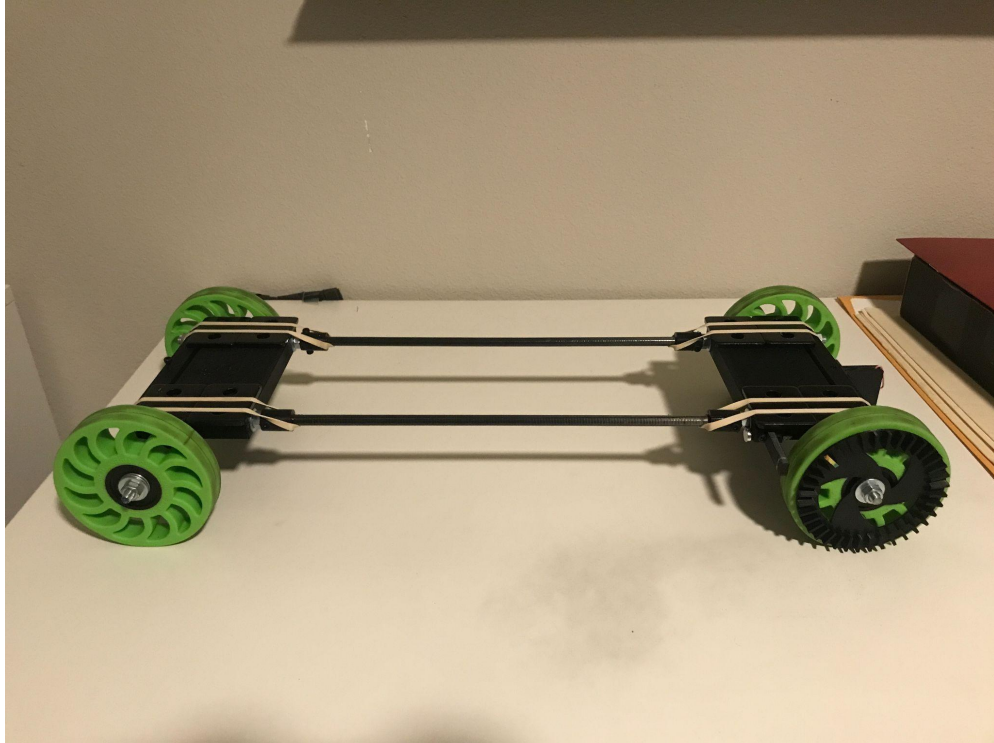


Figure 17: The V2 design

The two vehicles I have built so far, V1 (Figure 16) and V2 (Figure 17), consist of 3 main components:

- **Chassis and axle mount:** This is a large and robust 3D printed component that allows the axle assembly to be mounted onto the chassis itself.
- **Chassis frame:** These consist of two carbon fiber tubes and an adapter system to connect them to the chassis/axle mount.
- **Axle assembly:** Consists of the wheels, bearings, and threaded rod axle.

Chassis and axle mount

There are two of these: one for each axle in the front and back of the vehicle.

- This component was 3D printed using PLA filament at 30-40% infill and evolved significantly between V1 and V2.
- It serves to mount the axle assembly and has provision for mounting the chassis frame (carbon fiber rods).

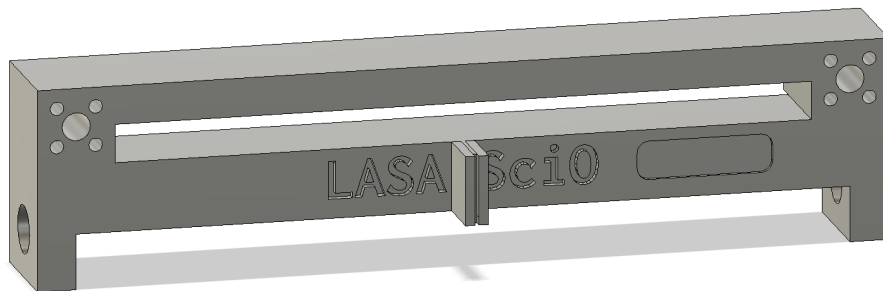


Figure 18: The V1 chassis and axle mount

- In Figure 18, the lateral hole cut into each side of the mount serves to house two flanged ball bearings (1/2" OD, 1/4" shaft ID).

- These holes are uniform and large enough to allow 1/4" hex nuts to pass through , and therefore do not allow an easy way of preventing lateral movement of the axle.
- The protrusion in front serves to mount a paperclip—the rules mandated method of measuring the vehicle's distance/accuracy from the target point.
- The 2 large holes coming in/out of the page serve to fit the carbon fiber rods of the chassis frame.
 - In V1, I did not have a robust method of securing these CF rods to the chassis mount, and simply used masking tape layers wrapped on each end of the tube to prevent slippage. This point, under high stress, eventually wore out.

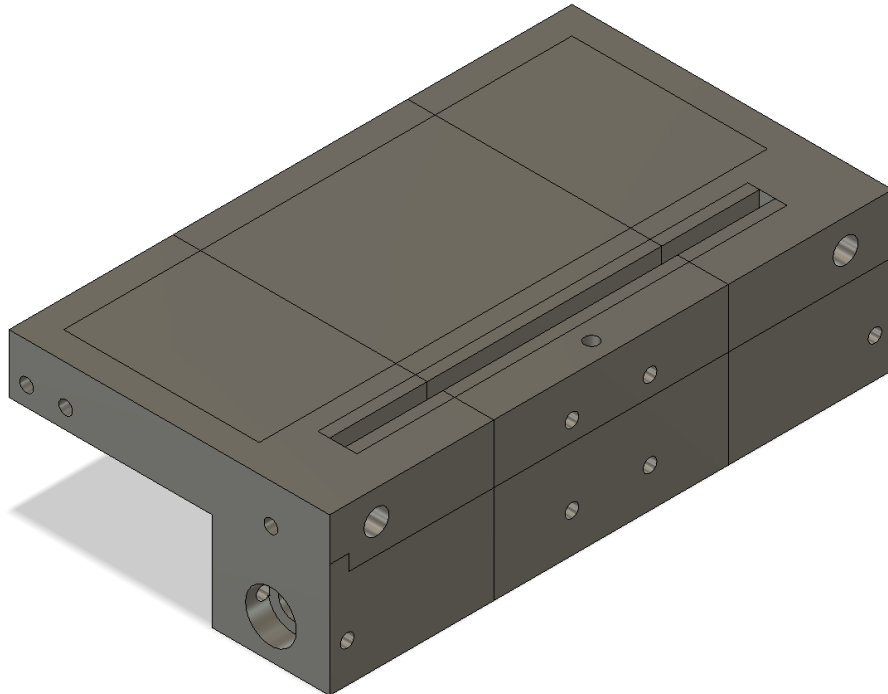


Figure 19: The V2 chassis and axle mount

- V2 (Fig. 19) mitigates these issues and offers improvement in other areas.
- The paperclip mount is removed and printed separately to reduce the use of printed supports and allow for convenient print positioning in slicing software.
- Further, the bearing hole is recessed, allowing for hex nuts on each side of the mount to be used to secure the axle laterally.
- When deciding the chassis width for V1 and V2, a key error was not to give consideration to the physics of the dowel obstacle. A smaller chassis width corresponds to a smaller axle track.
 - If an asymmetric impulse occurs on one of the wheels head-on, as would occur when the dowel is mounted, a longer track subjects the axle to greater angular impulse.
 - This would make the entire vehicle veer off in one direction following the dowel bump. This issue is fixed in V3.

Chassis frame

The frame consists of two 0.285" OD, 0.25" ID carbon fiber tubes that run perpendicular to the axes and link each of the above chassis mounts. In V1, a crude masking tape method was used to attach these tubes to the chassis mounts.

- A 3D printed cylindrical piece and 1/4" threaded rods were used in V2.
- As shown in Figure 20, the small sections of threaded rod extends into the chassis (not pictured), and is tightened with a pair of nuts to allow for adjustment.

- This established a precise way of calibrating the vehicle's lateral stability, or steering, when rolling forward at 4 different points, and also strengthened the overall structural integrity of the vehicle.



Figure 20: The two parallel CF rods, adapters, and threaded rods on each end

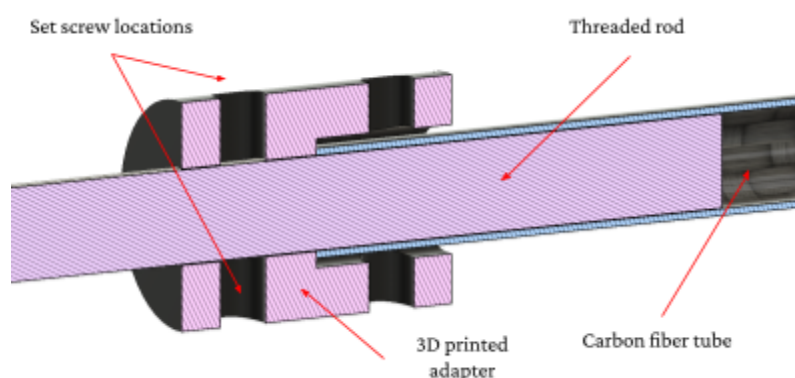


Figure 21: Cutaway of threaded rod to carbon fiber tube assembly

- The carbon fiber rod is secured to the large 3D printed cylindrical adapter using 2-part epoxy.
- The threaded rod is then fit into the adapter and extends a few centimeters into a hollow carbon tube to prevent wobble.
- 2 set screws are then placed in the 3D-printed adapter to secure the threaded rod.

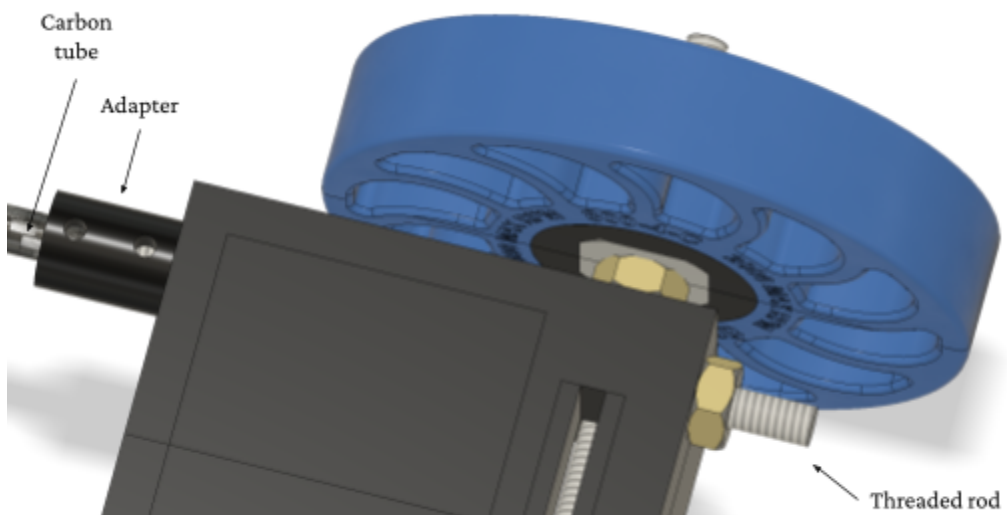


Figure 22: Close-up of the threaded rods entering the chassis

When deciding the vehicle's length, 2 factors must be considered:

- Physics of varying wheelbase lengths
- Ramp dimensions

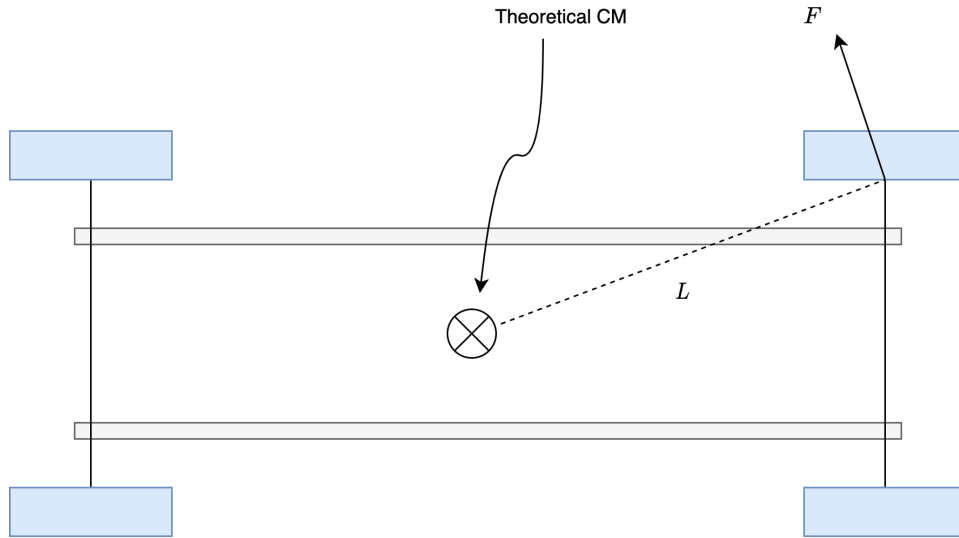


Figure 23: Vehicle turn behavior

A longer wheelbase means that each axle assembly is located further from the vehicle's center of mass (CM). When steering in one direction, the lateral steering force applied to the wheel is less when the moment arm from the CM to a wheel is larger.

- Thus, a larger wheelbase helps prevent the vehicle from laterally veering off course, especially when encountering the dowel, assuming the CM stays in the approximate center of the vehicle.
- However, the wheelbase is limited by the hypotenuse formed by connecting the two free vertices of the ramp (see Fig. 24).
- This steering behavior applies to both rear and front axles, so I decided to keep the CM in the approximate center to encourage similar steering behavior on the front and rear axles.
- It is important to note that W (below) is limited by the dimensions of the ramp itself.

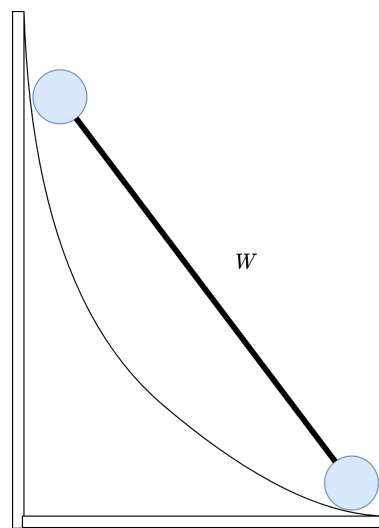


Figure 24: The maximum possible wheelbase, limited by ramp

Axle assembly



Figure 25: Wingnut braking mechanism

I decided that the most effective way of stopping the vehicle would be through a wingnut that ran along the axle, limited on two sides by the bearing to chassis mount attachment.

- As shown in Figure 25, the flat side of the wingnut rests against the chassis mount and runs towards the right edge as the wheel is spun in the forward direction.
- When it reaches the edge, the axle locks, halting the vehicle.



Figure 26: Metal weight plates on chassis mount

The vehicle's 2 kg weight limit was an important design clue.

- Greater mass concentrated above each axle "dampened" the bounce effect as the vehicle traveled over the dowel.
- The prototype V1 incorporated no such mass but I placed four ~50 g metal plates on each chassis, for a total of 8 plates (400 g).
- Total weight of V2 was ~1.4 kg (400 g weight + 1000 g empty weight of vehicle).
- In V3, I get as possible to the weight limit to mitigate the bounce effect, making adjustments to the braking mechanism if needed to prevent possible skidding.



Figure 27: [BaneBots T81 30A 4” wheel](#)

The wheels chosen, constant across V1 and V2, were 4” BaneBots T81 models with a 30A shore rating.

- I chose the softest wheels possible to allow for a shock-absorbing effect when encountering the bounce.
- Larger diameter wheels (4") were chosen in order to give greater ground clearance for the chassis and increase the “suspension” travel in the wheel’s crumple zones.

Ramp

My ramp (Figure 27) consists of two L-shaped pieces of plywood, joined with 90° angle brackets, that house a curved piece of tempered hardboard secured in each corner with a bolt.

- I chose to use a curved surface, as this would help the vehicle smoothly transition towards rolling on the level floor without an abrupt collision with the floor—an impulse that could cost energy better used to surpass the dowel obstacle.
- The shape of this curve is not important and was approximated during the build phase primarily with preserving structural integrity of the hardboard surface in mind.
 - Given a starting height, the vehicle will exit the ramp with the same velocity regardless of the shape, given that kinetic friction between the wheels and ramp surface is negligible.
 - The point of having a curved transition is to allow the vehicle to smoothly transition to the floor without losing its potential energy to unwanted impulses.



Figure 27: The ramp

The launch mechanism for the vehicle was kept as simple as possible in order to mitigate possible errors during launch. It consists of a 3D printed piece mounted to the ramp surface, with two vertically drilled holes.

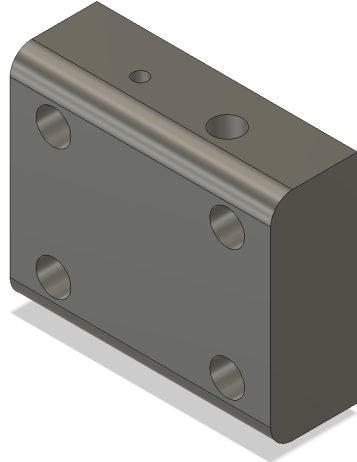


Figure 28: 3D render of the launch mount, note longitudinal holes for screw and pencil

One hole houses a small screw that secures one end of a length of sewing thread. The other hole houses a pencil, around which the other end of thread is secured in a small loop. The thread is then hooked to a screw on the rear of the vehicle. When the pencil is removed, the string quickly detaches from the vehicle and allows it to roll down the ramp (see Fig. 29).

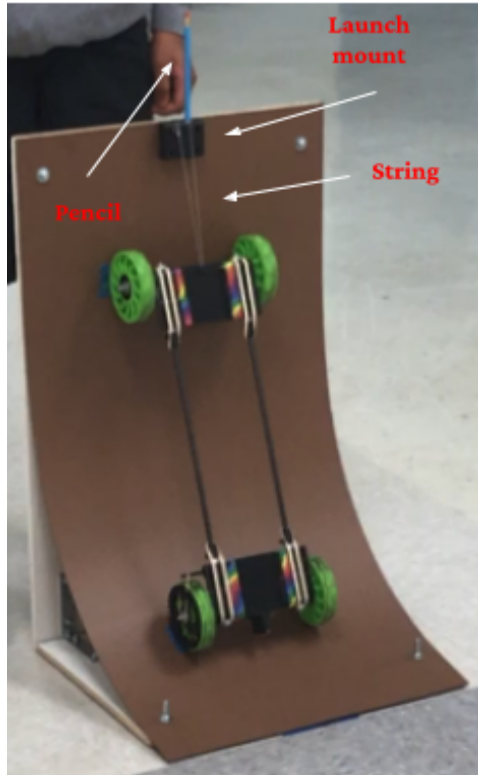


Figure 29: Overall view of the ramp launch mount and V2's hitch in launch position

Calibration

In order to precisely stop at the target point, it was necessary to establish a precise calibration system.

- Measuring the distance from the wingnut's flat end to the side of the chassis leaves significant room for error, necessitating the precise counting of wheel turns as a parameter.
- I attached a 3D-printed circular wheel (Fig. 30) to one of the tires with 36 protrusions, allowing for 10-degree calibration intervals of rotation.

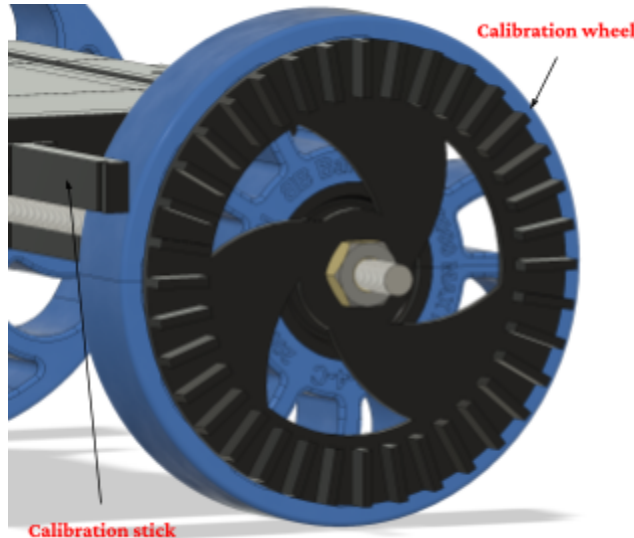


Figure 30: Calibration wheel and stick assembly on vehicle

The stick is used as a reference point to ensure that I set the right calibration metric each time, and a rubber band is attached to the stick and desired protrusion as a “parking brake” when I handle the vehicle.

I collected data over 14 trials in order to calibrate V2:

Trial	Wheel rotations (full.[n/36])	Actual rotations	Actual distance (cm)	Target distance (cm)
1	3	3.000	103.2	100
2	6	6.000	184	200
3	6.18	6.500	191.5	200
4	6.24	6.667	201.5	200
5	6.24	6.667	200.5	200
6	9	9.000	263.5	300
7	10	10.000	295.8	300
8	10.12	10.333	302.5	300
9	12	12.000	356.5	400
10	13.24	13.667	401.5	400
11	15	15.000	447	500

12	15.24	15.667	478.5	500
13	16	16.000	487.5	500
14	16.8	18.222	507	500

I attempted to calibrate the vehicle to whole numbered distance values of 2, 3, 4, and 5 meters as accurately as possible, with best results being between 0.5 and 5 centimeters from the target point. This produced a fairly reliable regression line plotting distance from the start point versus wheel rotations, with an R^2 of 0.993.

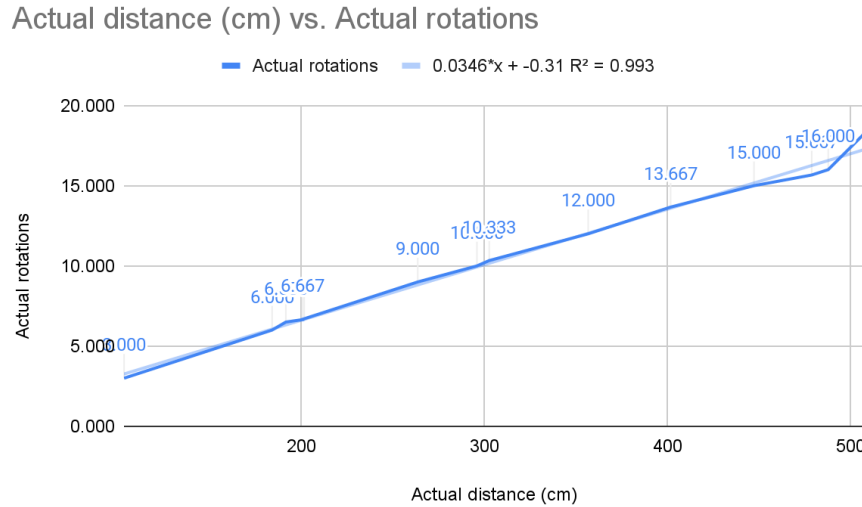


Figure 31: Data regression

Using the above equation of form $\hat{y} = ax + b$, I can plug in the provided target distance x at competition to obtain the theoretical number of rotations \hat{y} .

Materials

- Autodesk Fusion 360 for 3D design
- Ender 3 V2 3D printer with standard black PLA filament
- Carbon fiber tubes (0.25" ID, 0.285" OD) from Rockwest Composites
- Pre-machined parts from hardware stores: threaded rods, hex nuts, wingnut, washers, etc.
- BaneBots T81 wheels and hubs

Challenges

- The main challenge faced during the testing phase was alignment. Inconsistency, even within a degree, can lead the vehicle to hit the dowel at the wrong angle or veer off course from the imaginary track centerline. This will need to be mitigated with a reliable sighting system for the ramp and consistent method of aligning the vehicle on the ramp surface
- Surpassing the dowel is unpredictable if the vehicle tends to bounce. This will need to be solved with the aid of either suspension or enough weight centered above each axle.
- The vehicle itself needs to be robust. Ensuring every bolt is tightened and the plastic components do not wear down is important, just as one would maintain their real car.

V3 design

This is the latest iteration of the Gravity Vehicle, and distinguishes itself from prior designs through

- The use of magnetically damped shock absorbers → improve the vehicle's encounter with the dowel in order to keep it on course
- Reinforced chassis → a triangular cross section of 3 carbon fiber tubes bolted to each chassis block (rear and front), reinforced with spacer clamps
- Reduced track length & increased wheelbase → improve handling and obstacle mounting of the dowel
- Increase of the curb weight to nearly 2 kg using metal plates mounted above and to the side of the front/rear → increase potential energy, ability to resist the obstacle's impulse through greater momentum of the vehicle, and pronounce the suspension effect

As of the time of writing, the new vehicle has not been fully constructed in physical form. An interactive render of the below 3D model can be found [here](#).



Figure 31: Render of the V3 design

The new design divides the chassis block into two horizontal components.

- Each component contains an array of neodymium magnets with similar poles facing each other
- Two 1/4" brushed aluminum shafts run through the chassis pieces, aided by a sleeve bearing
- Two springs run along the shafts, acting as shock absorbers damped by the magnets.

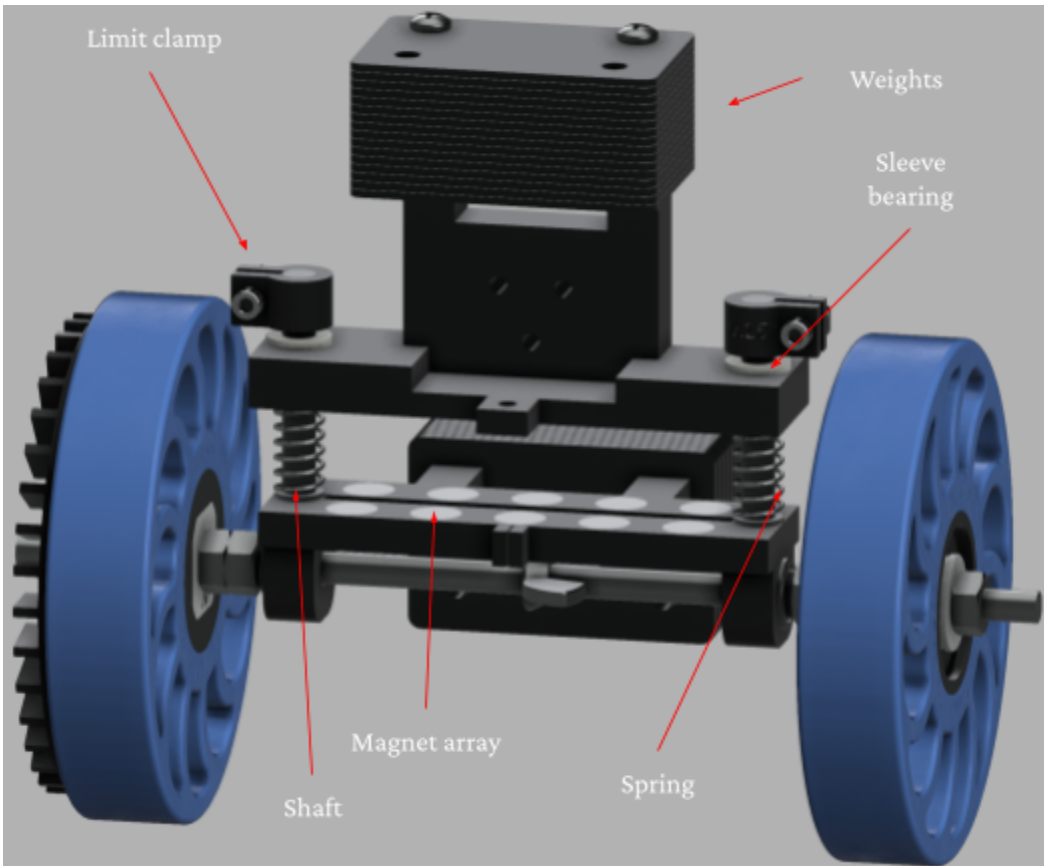


Figure 32: Front/rear chassis block and suspension close-up. Note spacer mounting holes below the vertical weight stack.

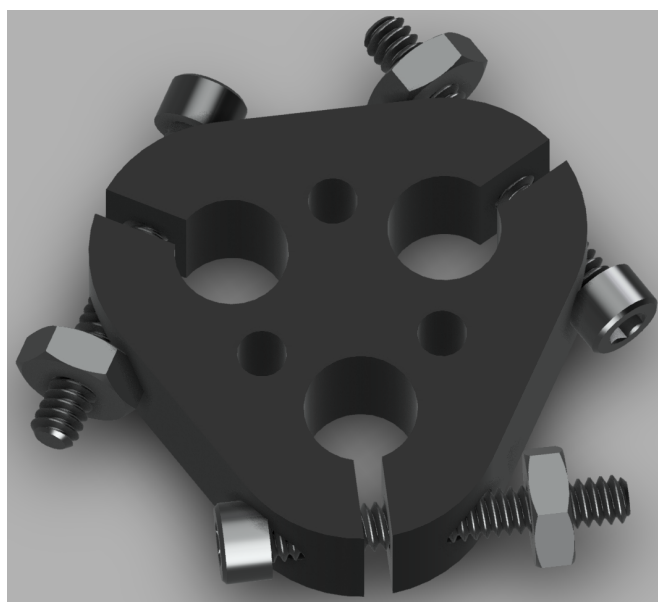


Figure 33: Spacer, with clamp screws and smaller bolt mounting holes